International Journal of Engineering

Journal Homepage: www.ije.ir

Effect of Magnetic Field on the Rotating Flow in a Similar Czochralski Configuration

S. Bouabdallah*, A. Atia, A. H. Boughzala

LME, Laboratory of Mechanics, Department of Mechanical Engineering, University of Laghouat, Road of Ghardaia, Laghouat, Algeria

PAPER INFO

Paper history:
Received 02November 2015
Received in revised form 30March 2016
Accepted 14 April 2016

Keywords:
Rotating Flow
Czochralski
Co-Counter-Rotating Mixed Convection
Magnetic Field

ABSTRACT

We present a numerical study of the rotating flow generated by two rotating disks in co-/counter-rotating, inside a fixed cylindrical enclosure similar to the Czochralski configuration (Cz). The enclosure having an aspect ratio $A = H/R_c$ equal to 2, filled with a low Prandtl number fluid (Pr = 0.011), which is submitted to a vertical temperature gradient. The finite volume method has been used to solve numerically the governing equations of the studied phenomenon.We present the steady state flow; and make a comparison between the flow generated by the co-/counter-rotating end disks. This study was caried out for different Richardson numbers; Ri = 0.01, 0.1, 0.5, 1, 2, 3, 5 and 10. The effect of orientation of the magnetic field is also taken into account for different values of the Hartmann number (Ha = 0, 5, 10, 20, 30 and 50). The obtained results show that the strongest stabilisation of the velocity field and heat transfer occurs when the flow generated byco-rotating end disks and the applied of magnetic field in radial direction provied a more stabilisation of the convective flow.

***doi**: 10.5829/idosi.ije.2016.29.04a.16*

NOMENCLATURE

A	aspect ratio $A = H/R_c$	Ri	Richardson number
B	intensity of magnetic field, Tesla	T	temperature, K
B_r	radial magnetic field, Tesla	U_r	dimensionless radial velocity
B_z	axial magnetic field, Tesla	U_z	dimensionless axial velocity
C_p	specific heat of liquid, J. kg^{-1}. K^{-1}	U_θ	dimensionless tangential velocity
F_{LR}	dimensionless Lorentz force in R-direction	**Greek Symbols**	
F_{LZ}	dimensionless Lorentz force in Z-direction	α	thermal diffusivity, m^2. s^{-1}
$F_{L\theta}$	dimensionless Lorentz force in θ-direction	β	thermal expansion coefficient, K^{-1}
g	gravitational acceleration, m. s^{-2}	δ	orientation of the magnetic field, °
Gr	Grashof number	Θ	dimensionless temperature
H	height of the cylinder, m	λ	thermal conductivity, W. m^{-1}. K^{-1}
Ha	Hartmann number	ρ	density of the fluid, kg. m^{-3}
Nu	local Nusselt number	σ	electric conductivity, Ω^{-1}.m^{-1}
Nu_{moy}	average Nusselt number	Ω	angular velocity, rad. s^{-1}
P	dimensionless pressure	Φ	dimensionless electric potential
Pr	Prandtl number	υ	kinematic viscosity, m^2.s^{-1}
R, Z	dimensionless meridional coordinates	**Subscripts**	
R_c	radius of the cylinder, m	c	cold
Re	Reynolds number	h	hot

[1]*Corresponding Author's Email: fibonsaid@gmail.com (S. Bouabdallah)

Please cite this article as:S. Bouabdallah, A. Atia, A. H. Boughzala,Effect of Magnetic Field on the Rotating Flow in a Similar Czochralski Configuration , International Journal of Engineering (IJE), TRANSACTIONS A: Basics Vol. 29, No. 4, (April 2016) 563-571

1. INTRODUCTION

Rotating flows with heat transfer in an enclosed cylinder driven by the rotation of the end wall and vertical gradient of temperature have been investigated by researchers for many years. This type of flows is presented in many practical situations as rotational viscosimeters, centrifugal machinery, pumping of liquid metals at high melting point and crystal growth from molten silicon in Cz crystal pullers [1]. The state of the art in this field has been summarized in [2, 3]. The first experiments by Vogel [4] and later by Escudier [5] showed the formation of a concentrated vortex core along the center axis. Based on their pioneering works, a lot of experimental and numerical studies have later been carried out. Among those, Spohn et al. [6] used the visualization techniques of electrolytic precipitation and showed that vortex breakdown bubbles in the container flow are open and asymmetric at their downstream end in the regime of axisymmetric bubbles. Recently, Sotiropoulos et al. [7] used planar laser induced fluorescence technique and showed the existence of chaotic behavior in the Lagrangian transport within the bubbles for flows that are steady from the Eulerian standpoint. In computations, there are numerous investigations of the container problem, for example, Lopez [8], Brown and Lopez [9]. All these studies were able to capture the flow evolution observed in the laboratory. They found that, the heat transfer rate increases with an increase of Re but it decreases with an increase of Ha. Rahimi and Yousefi [10] presented the transient laminar fluid mot ion and heat transfer resulting from the impulsive heating or cooling of a vertical surface in a quiescent fluid.Sheikhzadeh et al. [11] investigated numerically the effect of magnetic field on natural convection. Magnetic fields are crucial in non-intrusive flow control of electrically conducting melts in various physics of industrial significance, MHD pumps, and plasma and fusion technology. Rahmannezhad et al. [12] investigated numerically the effects of a magnetic field on mixedconvection of Al_2O_3-water nanofluid in a square lid-driven cavity. Continuous casting is this kind of process using different magnetic field configurations to control the flow of steel in the mold and further to promote efficiency and minimize defects [13]. For example, static [14], rotating and travelling magnetic fields [15, 16] provide attractive means for braking, stirring and mixing. When a magnetic field is applied on flow field, it induces a current and the interaction between this current and the magnetic field will generates a Lorentz force, this lettre alters the flow field. In case of swirling flow under a magnetic field, the phenomena are commonly seen in metallurgical MHD, such as in solidified ingot. The swirling flows usually maintain a stable laminar flow and a second flow, and are named Ekman pumping [17, 18]. The second flow is superimposed on the primary swirling flow. Ben Hadid et al. [19] studied the 3D oscillatory flow of a conducting molten metal confined in a cylindrical cavity. They examined the temporal signals, the properties of symmetry and the assessments of energy characterizing oscillatory flow, and the damping of the flow oscillatory by a vertical magnetic field until the stabilization of this flow. Talmage et al. [20] studied the rotational movement of the molten metal during the production of crystals of silicon by the Cz technique with a high, uniform, and vertical magnetic field. MHD flow of motlen Gallium during phase change in 3D enclosure was investigated [21]. In an enclosed cylinder [22] they simulated and sutided the influences of conductivity of the upper lid, lower base and side wall were investigated at Ha = 100 and Re = 100. The analytical solutions of the MHD flows for different electrical conductivity were presented and compared with the numerical results in [23]. Davidson et al. [24] studied Ekman pumping and Bödewadt-Hartmann layers in an axisymmetric pool and an open axisymmetric system, respectively. To the best of our knowledge, the effect of axial and radial magnetic field applied separately in rotating flow generated by the co/counter rotating end disks of the enclosed cylinder have never been studied, except for the case treated recently by Mahfoud and Bessaih [25], but with axial magnetic field applied. Therefore, the objective of this work is to study the effect of magnetic field orientations on rotating flow. This sutdy was carried out for $Ri \leq 10$, and for different intensities of magnetic field (Ha = 0, 5, 10, 20, 30 and 50).

2. PROBLEM DESCRIPTION AND MATHEMATICAL FORMULATION

The physical system under consideration Fig. 1, is a cylindrical enclosure has a radius R_c and height H, the aspect ratio is fixed ($A = H/R_c = 2$). The enclosure contains a liquid silicon (Pr = 0.011), the bottom disk is rotating with a constant angular velocity (+Ω), and maintained at a hot temperature T_h, while the top disk is in co-/counter-rotating and maintained at a cold temperature T_c (we called co-rotating flow when the two end disks rotate in the same direction with Ω, and counter-rotating flow for the opposite directions). The side wall of the cylinder is adiabatic. The system may be subjected to a magnetic field of constant magnitude B, oriented in both axial and radial directions, separately. Adopting the assumptions of [25], and introducing the scales R_c for lengths, ΩR_c for velocities, $\rho(\Omega R_c)^2$ for pressure, $(T_h - T_c)$ for temperature, and $\Omega R_c^2 B$ for electric potential, the dimensionless equations of the system become:

$$\frac{1}{R}\frac{\partial}{\partial R}(RU_r)+\frac{\partial U_z}{\partial Z}=0 \quad (1)$$

$$\frac{1}{R}\frac{\partial}{\partial R}(RU_r^2)+\frac{\partial}{\partial Z}(U_rU_z)+\frac{U_\theta^2}{R}=-\frac{\partial P}{\partial R}+\frac{1}{\mathrm{Re}}\left[\frac{1}{R}\frac{\partial}{\partial R}(R\frac{\partial U_r}{\partial R})+\frac{\partial^2U_r}{\partial Z^2}-\frac{U_r}{R^2}\right]+\frac{Ha^2}{\mathrm{Re}}F_{LR} \quad (2)$$

$$\frac{1}{R}\frac{\partial}{\partial R}(RU_rU_z)+\frac{\partial}{\partial Z}(U_z^2)=-\frac{\partial P}{\partial Z}+\frac{1}{\mathrm{Re}}\left[\frac{1}{R}\frac{\partial}{\partial R}(R\frac{\partial U_z}{\partial R})+\frac{\partial^2U_z}{\partial Z^2}\right]+Ri.\Theta+\frac{Ha^2}{\mathrm{Re}}F_{LZ} \quad (3)$$

$$\frac{1}{R}\frac{\partial}{\partial R}(RU_rU_\theta)+\frac{\partial}{\partial Z}(U_zU_\theta)+\frac{U_rU_\theta}{R}=\frac{Ha^2}{\mathrm{Re}}F_{L\theta}+\frac{1}{\mathrm{Re}}\left[\frac{1}{R}\frac{\partial}{\partial R}(R\frac{\partial U_\theta}{\partial R})+\frac{\partial^2U_\theta}{\partial Z^2}-\frac{U_\theta}{R^2}\right] \quad (4)$$

$$\frac{1}{R}\frac{\partial}{\partial R}(RU_r\Theta)+\frac{\partial}{\partial Z}(U_z\Theta)=\frac{1}{\mathrm{Pr}}\left[\frac{1}{R}\frac{\partial}{\partial R}(R\frac{\partial\Theta}{\partial R})+\frac{\partial^2\Theta}{\partial Z^2}\right] \quad (5)$$

where, F_{LR}, F_{LZ} and $F_{L\theta}$ are the Lorentz force component in *R*, *Z* and θ directions, respectively. Thier expressions were given as following:

- Case of axial magnetic field (B_z) :

$$F_{LR}=-U_r,\ F_{LZ}=0 \text{ and } F_{L\theta}=\frac{\partial\Phi}{\partial Z}-U_\theta \quad (6a)$$

- Case of radial magnetic field (B_r) :

$$F_{LR}=0,\ F_{LZ}=-U_Z \text{ and } F_{L\theta}=-\frac{\partial\Phi}{\partial Z}-U_\theta \quad (6b)$$

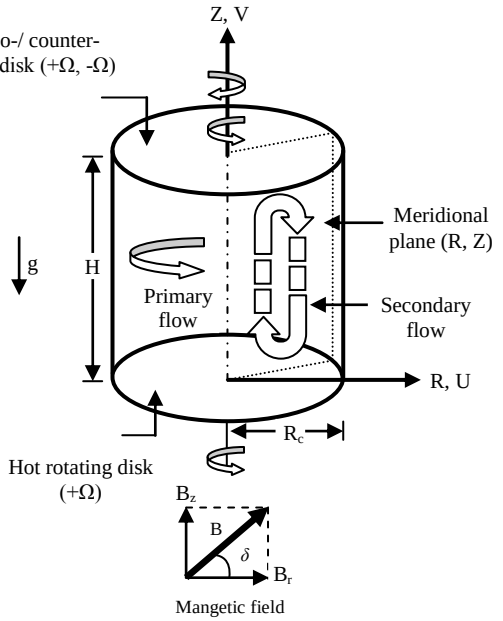

Figure 1. Sketch of physical problem.

The appear flow parameter in the dimensionless mathematical model are: Reynolds number $\mathrm{Re}=\Omega R^2/\upsilon$, Richardson number $Ri=Gr/\mathrm{Re}^2$, Grashof number $Gr=g\beta(T_h-T_c)R^3/\upsilon^2$, Prandtl number $\mathrm{Pr}=\upsilon/\alpha$ and Hartmann number $Ha=BR\sqrt{\sigma/\rho\upsilon}$ which is indicate the ratio between the electromagnetic force and viscosity force.

The boundary conditions are given as following:

At: $R=0$ and $0\le Z\le 2$:

$$U_r=U_\theta=\frac{\partial U_z}{\partial R}=0,\ \frac{\partial\Theta}{\partial R}=0\ \frac{\partial\Phi}{\partial R}=0 \quad (7a)$$

At: $R=1$ and $0\le Z\le 2$:

$$U_r=U_\theta=U_z=0,\ \frac{\partial\Theta}{\partial R}=0,\ \frac{\partial\Phi}{\partial R}=0 \quad (7b)$$

At: $Z=0$ and $0\le R\le 1$:

$$U_r=U_z=0,\ U_\theta=R\ ,\ \Theta=1,\ \frac{\partial\Phi}{\partial R}=0 \quad (7c)$$

- Co-rotation case

At: $Z=2$ and $0\le R\le 1$:

$$U_r=U_z=0,\ U_\theta=R\ ,\ \Theta=0\ ,\ \frac{\partial\Phi}{\partial R}=0 \quad (7d)$$

- Counter-rotation case

At: $Z=2$ and $0\le R\le 1$:

$$U_r=U_z=0,\ U_\theta=-R\ ,\ \Theta=0\ ,\frac{\partial\Phi}{\partial R}=0 \quad (7e)$$

3. NUMERICAL METHOD AND CODE VALIDATION

The mathematical model constructed by the Equations (1) to (5) and associated boundary conditions (Equations (7a) to (7e)) are resolved using the finite volume method by Ziapour et al. [26]. The scalar variables ($\Theta$and *P*) are stored at the middle of the volume; moreover the vector variables are stored at the faces of the control volume. The diffusion and convection terms are discretized by a second-order central difference scheme, and the SIMPLER Algorithm [27] is used to solve the coupled velocity-pressure. The Acquired algebraic equations are solved by TDMA. The convergence of computation was checked by the differences in flow parameter between two consecutive iteration that must be less than 10^{-5}. The used grid is not regular, we chosen the space increment according to geometric progressions as the same to the work of Atia et al. [28]. This grid refinement allows controlling the Hartmann layer developed at near the walls caused by

strong gradients of velocity and temperature. So, thus requiring a great number of nodes to solve the specific characteristics of the MHD flow, also in order to reduce the numerical errors [29]. To examine the effect of grid size on the numerical results, several grids were studied such as: 50×100, 60×120, 80×160 and 100×200. We consider the case of a mixed convection flow with Ri = 2. The computational results we directing to choice the grids 80×160, since the time of program execution for those of the grid (100×200) high than the chosen grid (the same computation domain was made in[25]).

To develop a constructive and objective comparison of the obtained results by our numerical simulations with experimental data, and to give interpretations to the observed phenomena, it is useful to validate our work. Firstly, a comparison with the results of Kakarantzas et al. [30] and Karcher et al. [31] was made. The author used a cylindrical enclosure have an aspect ratio equal to A = 4.125, and a fluid have Pr = 0.0203. The upper wall is hated electrically, moreover the bottom and lateral wall cooled by cycle water. The maximum value of the temperature versus Ha is presented in Fig. 2a. A good agreement between the obtained and reported results was observed. Secondly, a comparison of the radial velocity component U_r at R = 0.25, with experimental measurements obtained by Karcher et al. [31] for Ha = 0 (Figure 2b) has been carried out. It is clear that the computed values can be seen to be in excellent agreement with the data measurements.

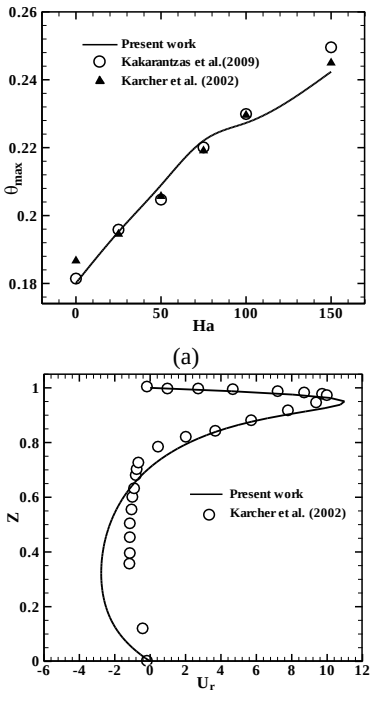

Figure 2. Comparison of our results with those of (a) Kakarantzas et al. [30] and (b) Karcher et al. [31].

4. RESULTS AND DISCUSSION

4. 1. Rotating Flow Without Magnetic Field We are interested herein to the behavior of the flow without magnetic field (Ha = 0). Equations (1) to (5), are solved numerically, without taking into account the Lorentz forces F_{LR} , F_{LZ} , $F_{L\theta}$ in the Navier–Stokes equations.

4. 1. 1. Co-rotation Case By carefully examining the results presented in Figure 3, it is noted that for all Ri the flow is multicellular. Particularly for $Ri \leq 1$, the flow is bi-cellular, we note also the presence of the Eckman layer in the area under the rotating disks is characterized by the large mass flow. These cells form opposing structures and the fluid in the bulk of the cylinder rotates almost rigidly with an intermediate velocity of the end disks, and due to the forced convection created by the rotation of the disks which dominates in this range. An inter-disk shear flow is created. These results are in good agreement with those of Omi and Iwatsu [32] with the creation of the meridional circulation. We note also that for the co-rotating case the stream function contours are nearly symmetrical about the mid-plane Z=1. When increasing Ri (Ri> 1) we can see that the cell background is increasing in size, either in intensity until the appearance of a secondary cell rotating within the main flow, by against the cell at the top is reduced until the occurrence of another recirculation zone adjacent to the side wall.

4. 1. 2. Counter-rotation Case Figure 4 shows the dimensionless streamlines for various Ri for the case of counter-rotating end disks. Almost the same comment as the disks rotates in co-rotation. We note that for all Ri the flow is multicellular, there is also an opposite flow than the first case of co-rotating, wherein for $Ri \leq 0.5$, we can see a symmetric situation. In which, each disk tends to cause a half thickness of fluid relative angular velocity (+Ω, -Ω). For Ri> 0.5, we note that the symmetry of the base flow is gone, and Ekman layers formed on the two rotary disks, a cell high capacity located near bottom wall, followed by a small cell near upper wall with the appearance of a side of the side wall cell (cells detachment) for Ri = 2 and Ri = 5, these emerging cells due to the acceleration of velocity of the fluid particles. For Ri> 0.5, we note that the symmetry of the base flow is gone, and the Ekman layers formed on the two rotary disks, a cell high capacity located near bottom wall, followed by a small cell near upper wall with the appearance of a side of the side wall cell (cells detachment) for Ri = 2 and Ri = 5, these emerging cells due to the acceleration of velocity of the fluid particles.

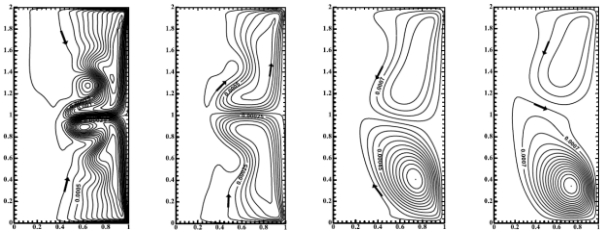

(a) Ri = 0.01 Ψmax= 1.35×10^{-3} (b) Ri = 0.1 Ψmax= 7×10^{-4} (c) Ri = 0.5 Ψmax= 8.5×10^{-4} (d) Ri = 1 Ψmax= 9.5×10^{-4}

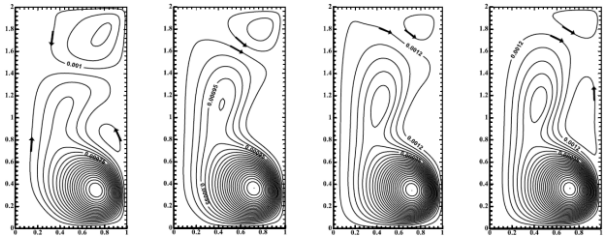

(e) Ri = 2 Ψmax= 1.15×10^{-3} (f) Ri = 3 Ψmax= 1.25×10^{-3} (g) Ri = 5 Ψmax= 1.3×10^{-3} (h) Ri = 10 Ψmax= 1.3×10^{-3}

Figure 3. Streamlines in R-Z plane, for different values of Ri. Case of co-rotating disks (without magnetic field).

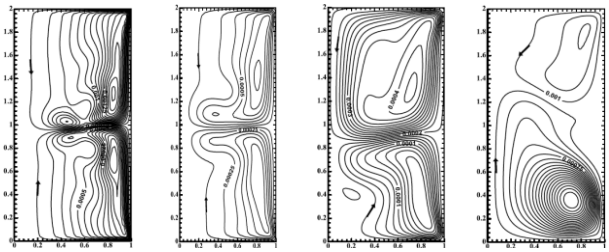

a) Ri = 0.01 Ψmax = 1.5×10^{-3} (b) Ri = 0.1 Ψmax = 7×10^{-4} (c) Ri = 0.5 Ψmax = 4.4×10^{-4} (d) Ri = 1 Ψmax = 1.15×10^{-3}

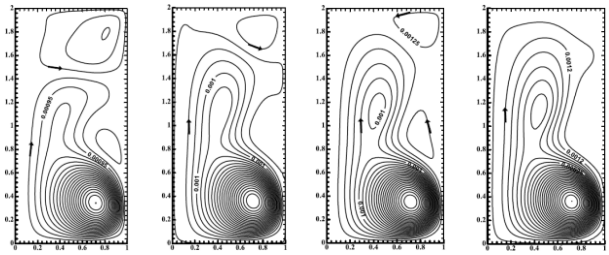

(e) Ri = 2 Ψmax = 1.2×10^{-3} (f) Ri = 3 Ψmax = 1.25×10^{-3} (g) Ri = 5 Ψmax = 1.3×10^{-3} (h) Ri = 10 Ψmax = 1.3×10^{-3}

Figure 4. Streamlines in R-Z plane, for different values of Ri. Case of counter-rotating disks (without magnetic field).

4. 2. Rotating Flow With Magnetic Field The application of a magnetic field is known about the stability of convective flows [19, 33]. If the electrical conducting fluid subjected to the magnetic field, the Lorentz force also was activated (the heat convection was provided by the combined action of buoyancy and the Lorenz force). This letters interrupted with the buoyancy force and change the heat and flow field. The magnetic field intensity and its orientation are the important factor they be affected on the velocity flow and the heat transfer rate.

4. 2. 1. Case of Co-rotating Disks Under the Axial Magnetic Field (δ = 90°) We fixed the magnetic field orientation at the angle δ = 90°. In Figure 5 (a-c), we present the streamlines for *Ri* = 0.5 and 10 respectively, and for different Ha. For low magnetic field (*Ha* = 10), it is clear that the relevant figure shows no change in the flow structure. But from *Ha* = 20, the latter starts to change, by the expansion of the cells which is a clear and significant change gradually as Ha increases. For *Ri* = 0.5, we note the presence of the Ekman layer on the two rotating disks, such that the main cell near hot lower rotary disk occupies almost all of the cylinder volume. For *Ri* = 10, the flow occurs more organized than the increasing of magnetic field intensity eliminates the small cells which nascent recirculation due to the acceleration of fluid particles. These changes due to electromagnetic forces .

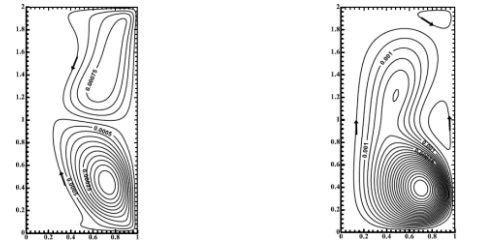

Ri = 0.5 $\Psi_{max} = 8\times10^{-4}$ *Ri* = 10 $\Psi_{max} = 1.2\times10^{-3}$

(a) *Ha* = 10

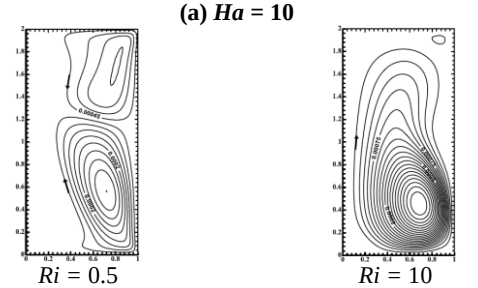

Ri = 0.5 $\Psi_{max} = 6.5\times10^{-4}$ *Ri* = 10 $\Psi_{max} = 1.05\times10^{-3}$

(b) *Ha* = 20

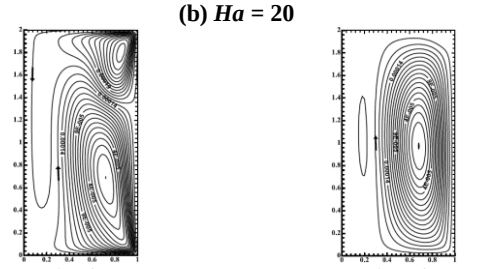

Ri = 0.5 $\Psi_{max} = 2.8\times10^{-4}$ *Ri* = 10 $\Psi_{max} = 1.9\times10^{-4}$

(c) *Ha* = 50

Figure 5. Streamlines in *R-Z* plane, for different values of Hartmann number (*Ri* = 0.5 and 10). Case of co-rotating disks (The magnetic field is applied in axial direction).

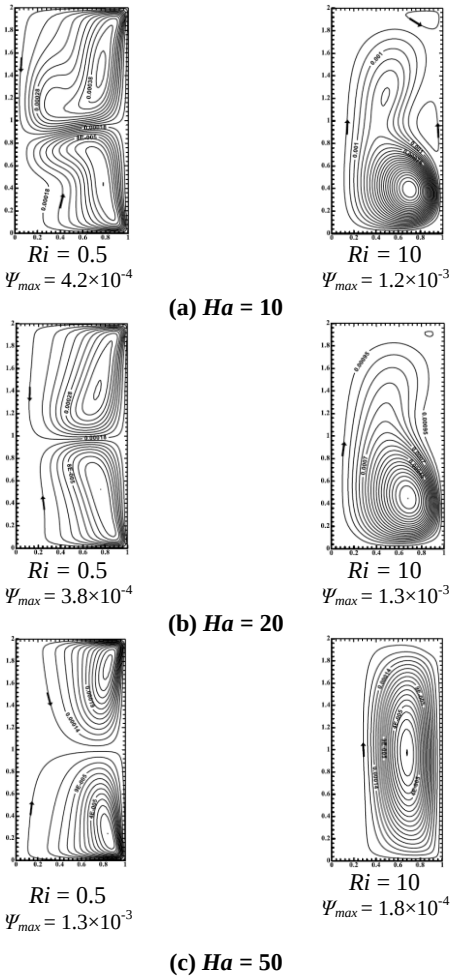

Figure 6. Streamlines in *R-Z* plane, for different values of Hartmann (*Ri* = 0.5 and 10). Case of counter-rotating disks (The magnetic field is applied in axial direction).

4. 2. 2. Case of Counter-rotating Disks Under the Axial Magnetic Field (δ = 90°) In Figure 6 (a-c), we presented the streamlines for *Ri* = 0.5 and 10 under the axial magnetic field, *Ha* = 10. We note that the flow structure has undergone a slight variation despite that we have increased Ha of at 10, the flow structure begins to change from Ha is set *Ha* = 20, by the expansion of the cells which is a clear and significant change gradually as *Ha* increases, Indeed, *Ha* = 50 the flow is more regular. We can connect this deformation to increasing of Ha, so the flow becomes more organized by the electromagnetic force which affects the fluid particles. It is notified also the presence of the Ekman layer for *Ri* = 0.5 located on the two rotating disks and the fluid in which each disk tends to cause a fluid to split-thickness relative angular velocity, at sufficiently high velocity the shear layer between the disk may become unstable, and wrap according vortex lines oriented radially the magnetic fields will be able to absorb the disturbance (Omi and Iwatsu[32]).To see a more information about the intensity of axial magnetic field B_z on the co-/counter-rotating flow, we have summarized in the Table 1.

4. 2. 3. Case of Co-rotatingDisks Under the Radial Magnetic Field (δ = 0°) In Figure 7 (a-c), we present the streamline for *Ri* = 0.5 and 10, and for different Ha (radial magnetic field). The change in the flow structures is started from *Ha*= 5; the cells are expanded gradually with increasing Ha. Then, for *Ha* ≥ 20 and *Ri* = 0.5 the flow becomes symmetric with respect to the mid-plane *Z* = 1. However, for *Ha* ≥ 20 and *Ri* = 10 we can see a reverse flow where the lower main cell increases gradually as higher cell and occupied the most volume of the cavity at *Ha* = 50. These changes show the magnetic stability. In addition, the effect of the radial magnetic field on the flow is more reliable than the axial magnetic field where we see a more different structure stable.

4. 2. 4. Case of Counter-rotatingDisks Under the Radial Magnetic Field (δ = 0°) For the case of counter-rotating disks in the presence of radial magnetic field, we present the streamlines for *Ri* = 0.5 and 10, and for different Ha (Figure 8 (a-c)). It is notified that a small variation on the flow structure is done when increases Ha at *5* the clear change on the flow structure starts from *Ha= 20* by expansion of cells (size/intensity) which is a significant change with successive increase of Ha. For *Ri* = 10, these cells are occupied almost the entire volume of the cavity. Noting that the effect of the radial magnetic field on the flow is lower for the Ri increases (*Ri* = 10) which shows an important effect of the magnetic field on flows dominated by natural convection (*Ri*> 1). Table 2, present the flow characteristic for different Ha. The magnetic field is applied in radial direction B_r (*Ri* = 0.5 and 10). We can conclude that the increase of *Ha* provides the decrease in the stream function and also for average Nusselt number. So, the rotating flow stabilizes when the intensity of radial magnetic field incresed.

TABLE. 1. Flow characteristic for different Ha in two case co-/ counter-rotating disks (axial magnetic field B_z).

Parameters		$\psi_{\max}$		Nu_{moy}	
Ha	*Ri*	Co-rotating	Counter-rotating	Co-rotating	Counter-rotating
0	0.5	4.4×10^{-4}	8.5×10^{-5}	1.419	1.422
	10	1.3×10^{-3}	1.3×10^{-3}	1.292	1.296
5	0.5	8.5×10^{-4}	4.2×10^{-4}	1.412	1.420
	10	1.3×10^{-3}	1.3×10^{-3}	1.290	1.292
10	0.5	8×10^{-4}	4.2×10^{-3}	1.404	1.416
	10	1.2×10^{-3}	1.2×10^{-3}	1.281	1.289
20	0.5	6.5×10^{-4}	3.8×10^{-4}	1.397	1.411
	10	1.05×10^{-3}	1.05×10^{-3}	1.276	1.285
50	0.5	2.8×10^{-4}	2.5×10^{-4}	1.367	1.399
	10	9×10^{-4}	1.8×10^{-4}	1.250	1.269

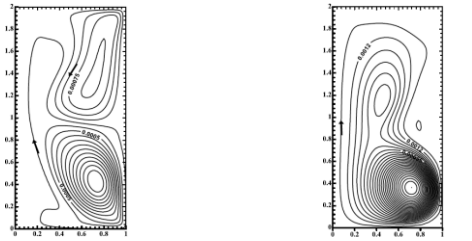

Ri = 0.5 $\Psi_{max} = 8.5\times10^{-4}$ | *Ri* = 10 $\Psi_{max} = 1.35\times10^{-3}$

(a) *Ha* = 5

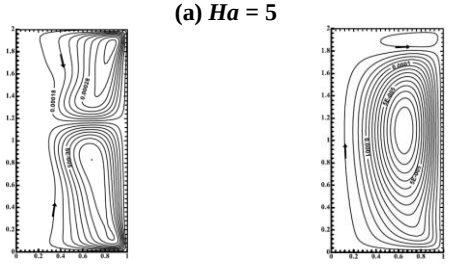

Ri = 0.5 $\Psi_{max} = 3.4\times10^{-4}$ | *Ri* = 10 $\Psi_{max} = 1.6\times10^{-4}$

(b) *Ha* = 20

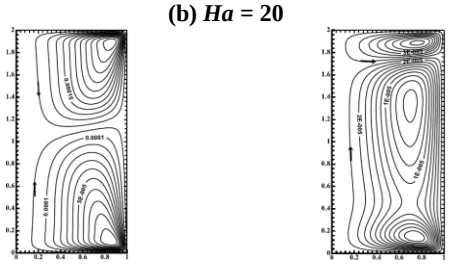

Ri = 0.5 $\Psi_{max} = 2.3\times10^{-4}$ | *Ri* = 10 $\Psi_{max} = 4\times10^{-5}$

(c) *Ha* = 50

Figure 7. Streamlines in *R-Z* plane, for different values of the Hartmann number (*Ri* = 0.5 and 10). Case of co-rotating disks (The magnetic field is applied in radial direction).

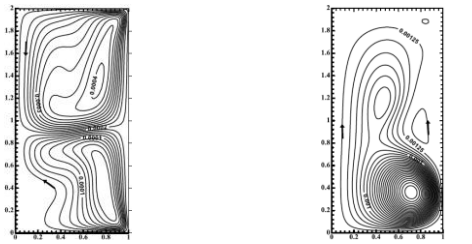

Ri = 0.5 $\Psi_{max} = 4.2\times10^{-4}$ | *Ri* = 10 $\Psi_{max} = 1.35\times10^{-3}$

(a) *Ha* = 5

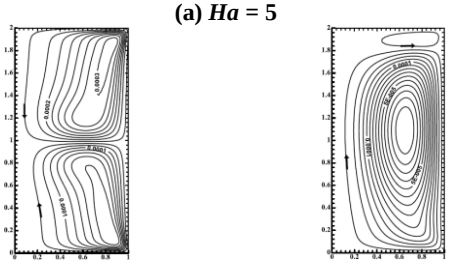

Ri = 0.5 $\Psi_{max} = 3.2\times10^{-4}$ | *Ri* = 10 $\Psi_{max} = 1.6\times10^{-4}$

(b) *Ha* = 20

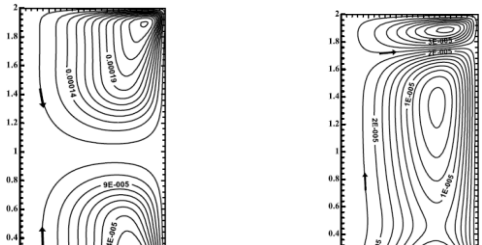

Ri = 0.5 $\Psi_{max} = 2.4\times10^{-4}$ | *Ri* = 10 $\Psi_{max} = 4\times10^{-5}$

(c) *Ha* = 50

Figure 8. Streamlines in *R-Z* plane, for different values of the Hartmann (*Ri* = 0.5 and 10). Case of counter-rotating disks (The magnetic field is applied in radial direction).

TABLE. 2. Flow characteristic for different Ha in two case co-/ counter-rotating case (radial magnetic field B_r).

Parameters		$\psi_{\max}$		Nu_{moy}	
Ha	***Ri***	**Co-rotating**	**counter-rotating**	**Co-rotating**	**counter-rotating**
0	0.5	4.4×10^{-4}	8.5×10^{-5}	1.419	1.422
	10	1.3×10^{-3}	1.3×10^{-3}	1.292	1.296
5	0.5	8.5×10^{-4}	4.2×10^{-4}	1.411	1.420
	10	1.35×10^{-3}	1.35×10^{-3}	1.290	1.291
10	0.5	6.5×10^{-4}	3.8×10^{-4}	1.402	1.415
	10	1.1×10^{-3}	1.1×10^{-3}	1.278	1.287
20	0.5	3.4×10^{-4}	3.2×10^{-4}	1.391	1.408
	10	1.6×10^{-4}	1.6×10^{-4}	1.272	1.280
50	0.5	2.3×10^{-4}	2.4×10^{-4}	1.360	1.390
	10	4×10^{-5}	4×10^{-5}	1.243	1.261

4. 2. 5. Comparison Between Two Cases Co-/Counter-rotating Disks With Magnetic Field In Table 2, we made comparison bewteen two cases.We can see that, the increase of Ha provides the decrease of the flow intensity in the two cases, but more important in the counter-rotating disks. We can also see the application of $B_r$can slow better than the application of B_z (Figure 9). This is for *Ri* = 0.5 and 10, and for two orientations of magnetic field (*Ha* = 50). We can see that the application of the magnetic field causes a decrease in the local Nusselt number, and the best stabilization is found for B_r .

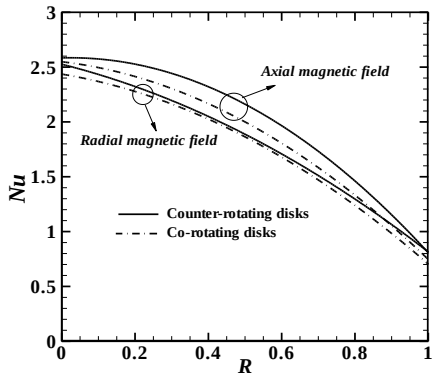

(a)

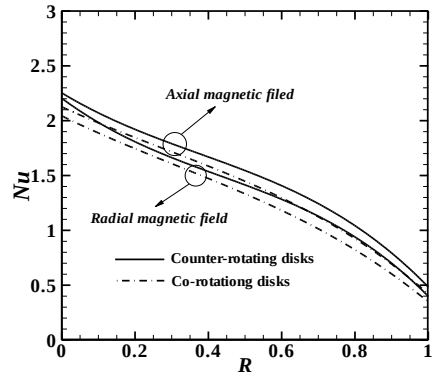

(b)

Figure 9. Effect of magnetic field orientation (Ha = 30) on the local Nusselt number: (a) Ri = 0.5, (b) Ri = 10.

5. CONCLUSIONS

A numerical study of the rotating flow generated by two rotating disks in co-/counter-rotating direction, inside a cylindrical enclosure similar to Cz configuration was carried out. Comparisons with published work on specific cases are performed and found to be in good agreement. From the obtained results, the following conclusions are drawn:

- The increase of Ri affects straightly on the structure of the flow in both cases co-/counter-rotation, wherever the velocity field and heat transfer rate are destabilized.
- The comparison between the flow generated by the co-rotating and counter-rotating disks shows that the strongest stabilization of the velocity field and heat transfer occurs when the flow generated by co-rotating end disks.
- In the presence of the magnetic field, the flow is more regular. An increase in the intensity of the magnetic field causes a change in the magnitude and flow structure, where is stabilize the velocity field and heat transfer rate.
- The magnetic field stabilization is important for the case of dominated natural convection (Ri >1).
- A more reduction of the velocity field and heat transfer rate is important when the radial magnetic field is applied (B_r).

6. REFERENCES

1. Tsitverblit, N. and Kit, E., "Numerical study of axisymmetric vortex breakdown in an annulus", ***Acta Mechanica***, Vol. 118, No. 1-4, (1996), 79-95.
2. Kharicha, A., Alemany, A. and Bornas, D., "Influence of the magnetic field and the conductance ratio on the mass transfer rotating lid driven flow", ***International Journal of Heat and Mass Transfer***, Vol. 47, No. 8, (2004), 1997-2014.
3. Granger, R., "Introduction to vortex dynamics", ***V. Karman Institute Lecture Series***, Vol. 8, (1986), 158-167.
4. Vogel, H.U., "Experimentelle ergebnisse über die laminare strömung in einem zylindrischen gehäuse mit darin rotierender scheibe", MPIStrömungsforschung, (1968), 342-350.
5. Escudier, M., "Observations of the flow produced in a cylindrical container by a rotating endwall", ***Experiments in fluids***, Vol. 2, No. 4, (1984), 189-196.
6. Spohn, A., Mory, M. and Hopfinger, E., "Experiments on vortex breakdown in a confined flow generated by a rotating disc", ***Journal of Fluid Mechanics***, Vol. 370, (1998), 73-99.
7. Sotiropoulos, F., Webster, D.R. and Lackey, T.C., "Experiments on lagrangian transport in steady vortex-breakdown bubbles in a confined swirling flow", ***Journal of Fluid Mechanics***, Vol. 466, (2002), 215-248.
8. Lopez, J., "Axisymmetric vortex breakdown part 1. Confined swirling flow", ***Journal of Fluid Mechanics***, Vol. 221, (1990), 533-552.
9. Brown, G. and Lopez, J., "Axisymmetric vortex breakdown part 2. Physical mechanisms", ***Journal of Fluid Mechanics***, Vol. 221, (1990), 553-576.
10. Baradaran Rahimi, A. and Yousefi, E., "Transient natural convection flow on an isothermal vertical wall at high prandtl numbers: Second-order approximation", ***International Journal of Engineering***, Vol. 14, No. 4, (2001), 367-376.
11. Sheikhzadeh, G., Babaei, M., Rahmany, V. and Mehrabian, M., "The effects of an imposed magnetic field on natural convection in a tilted cavity with partially active vertical walls: Numerical approach", ***International Journal of Engineering-Transactions A: Basics***, Vol. 23, No. 1, (2009), 65-78.
12. Rahmannezhad, J., Ramezani, A. and Kalteh, M., "Numerical investigation of magnetic field effects on mixed convection flow in a nanofluid-filled lid-driven cavity", ***International Journal of Engineering Trans. A: Basics***, Vol. 26, (2013), 1213-1224.
13. Davidson, P., "Magnetohydrodynamics in materials processing", ***Annual Review of Fluid Mechanics***, Vol. 31, No. 1, (1999), 273-300.
14. Tian, X.-Y., Zou, F., Li, B.-W. and He, J.-C., "Numerical analysis of coupled fluid flow, heat transfer and macroscopic solidification in the thin slab funnel shape mold with a new type embr", ***Metallurgical and Materials Transactions B***, Vol. 41, No. 1, (2010), 112-120.
15. Cramer, A., Pal, J. and Gerbeth, G., "Experimental investigation of a flow driven by a combination of a rotating and a traveling magnetic field", ***Physics of Fluids (1994-present)***, Vol. 19, No. 11, (2007), 109-118.
16. Koal, K., Stiller, J. and Grundmann, R., "Linear and nonlinear instability in a cylindrical enclosure caused by a rotating magnetic field", ***Physics of Fluids (1994-present)***, Vol. 19, No. 8, (2007), 88-107.

17. Moreau, R.J., "Magnetohydrodynamics, Springer Science & Business Media, Vol. 3, (2013).
18. Davidson, P., Kinnear, D., Lingwood, R., Short, D. and He, X., "The role of ekman pumping and the dominance of swirl in confined flows driven by lorentz forces", ***European Journal of Mechanics-B/Fluids***, Vol. 18, No. 4, (1999), 693-711.
19. Ben Hadid, H., Henry, D. and Touihri, R., "Unsteady 3d buoyancy-driven convection in a circular cylindrical cavity and its damping by magnetic field", ***Journal of Crystal Growth***, Vol. 180, No. 3-4, (1997), 433-441.
20. Talmage, G., Shyu, S.-H., Walker, J. and Lopez, J., "Inertial effects in the rotationally driven melt motion during the czochralski growth of silicon crystals with a strong axial magnetic field", ***Zeitschrift Fur Angewandte Mathematik Und Physik ZAMP***, Vol. 51, No. 2, (2000), 267-289.
21. Bouabdallah, S. and Bessaih, R., "Magnetohydrodynamics stability of natural convection during phase change of molten gallium in a three-dimensional enclosure", ***Fluid Dynamics & Materials Processing***, Vol. 6, No. 3, (2010), 251-276.
22. Mahfoud, B. and Bessaïh, R., "Stability of swirling flows with heat transfer in a cylindrical enclosure with co/counter-rotating end disks under an axial magnetic field", ***Numerical Heat Transfer, Part A: Applications***, Vol. 61, No. 6, (2012), 463-482.
23. Bessaih, R., Marty, P. and Kadja, M., "Hydrodynamics and heat transfer in disk driven rotating flow under axial magnetic field", ***International Journal of Transport Phenomena***, Vol. 5, No., (2003), 259-278.
24. Davidson, P. and Pothérat, A., "A note on bödewadt–hartmann layers", ***European Journal of Mechanics-B/Fluids***, Vol. 21, No. 5, (2002), 545-559.
25. Mahfoud, B. and Bessaih, R., "Oscillatory swirling flows in a cylindrical enclosure with co-/counter-rotating end disks submitted to a vertical temperature gradient", ***Fluid Dynamics & Materials Processing***, Vol. 8, No. 1, (2012), 1-26.
26. Ziapour, B.M. and Rahimi, F., "Numerical study of natural convection heat transfer in a horizontal wavy absorber solar collector based on the second law analysis", ***International Journal of Engineering***, Vol. 29, No. 1, (2016), 109-117.
27. Patankar, S., "Numerical heat transfer and fluid flow, CRC press, (1980).
28. Atia, A., Bouabdallah, S., Teggar, M. and Benchatti, A., "Numerical study of mixed convection in cylindrical czochralski configuration for crystal growth of silicon", ***International Journal of Heat and Technology***, Vol. 33, No. 1, (2015), 39-46.
29. Wang, B.-F., Ma, D.-J., Guo, Z.-W. and Sun, D.-J., "Linear instability analysis of rayleigh–bénard convection in a cylinder with traveling magnetic field", ***Journal of Crystal Growth***, Vol. 400, (2014), 49-53.
30. Kakarantzas, S., Sarris, I., Grecos, A. and Vlachos, N., "Magnetohydrodynamic natural convection in a vertical cylindrical cavity with sinusoidal upper wall temperature", ***International Journal of Heat and Mass Transfer***, Vol. 52, No. 1, (2009), 250-259.
31. Karcher, C., Kolesnikov, Y., Andreev, O. and Thess, A., "Natural convection in a liquid metal heated from above and influenced by a magnetic field", ***European Journal of Mechanics-B/Fluids***, Vol. 21, No. 1, (2002), 75-90.
32. Omi, Y. and Iwatsu, R., "Numerical study of swirling flows in a cylindrical container with co-/counter-rotating end disks under stable temperature difference", ***International Journal of Heat and Mass Transfer***, Vol. 48, No. 23, (2005), 4854-4866.
33. Bouabdallah, S. and Bessaïh, R., "Effect of magnetic field on 3d flow and heat transfer during solidification from a melt", ***International Journal of Heat and Fluid Flow***, Vol. 37, (2012), 154-166.

Effect of Magnetic Field on the Rotating Flow in a Similar Czochralski Configuration

S. Bouabdallah, A. Atia, A. H. Boughzala

LME, Laboratory of Mechanics, Department of Mechanical Engineering, University of Laghouat, Road of Ghardaia, Laghouat, Algeria

P A P E R I N F O

Paper history:
Received 02 November 2015
Received in revised form 30March 2016
Accepted 14 April 2016

Keywords:
Rotating Flow
Czochralski
Co-Counter-Rotating Mixed Convection
Magnetic Field

چکیده

ما در حال حاضر، مطالعه عددی جریان چرخشی تولید شده را توسط دو دیسک چرخشی در چرخش همسو/ ناهمسو، در داخل محوطه یک استوانه ثابت مشابه پیکربندی Czochralski (Cz) نشان می دهیم. محوطه دارای نسبت A = H / RC برابر با ۲، پر شده با سیالی با عدد پرانتل کوچک (Pr =۰/۰۱) می باشد که به گرادیان دما عمودی نسبت داده می شود. روش حجم محدود برای حل عددی معادلات حاکم پدیده تحت مطالعه استفاده شده است. ما جریان حالت پایدار را ارائه می دهیم؛ و مقایسه ای بین جریان تولید شده توسط دیسک های انتهایی با چرخش همسو/ناهمسو نشان می دهیم. این مطالعه برای عددهای مختلف ریچاردسون Ri برابر با ۰/۰۱، ۰/۱، ۰/۵، ۱، ۲، ۳، ۵ و ۱۰ انجام شد. اثر جهت میدان مغناطیسی نیز برای مقادیر مختلف عدد هارتمن Ha برابر با ۰، ۵، ۱۰، ۲۰، ۳۰ و ۵۰ به حساب می آید. نتایج به دست آمده نشان می دهد که قوی ترین تثبیت میدان سرعت و انتقال حرارت هنگامی رخ میدهد که جریان، دیسک های انتهایی چرخش byco تولید می کند و اعمال میدان مغناطیسی در جهت شعاعی، ثبات بیشتری از جریان همرفتی را ایجاد می کند.

***doi**: 10.5829/idosi.ije.2016.29.04a.16*